Processing and Application of Ceramics 13 [1] (2019) 104–113
https://doi.org/10.2298/PAC1901104D

Magneto-dielectric properties of ferrites and ferrite/ferroelectric multiferroic composites

Adis S. Džunuzović*, Mirjana M. Vijatović Petrović, Nikola I. Ilić, Jelena D. Bobić, Biljana D. Stojanović

Institute for Multidisciplinary Research University of Belgrade, Kneza Višeslava 1, Belgrade, Serbia

Received 10 October 2018; Received in revised form 27 December 2018; Accepted 12 March 2019

Abstract

Ni-Zn ferrites, with the general formula $Ni_{1-x}Zn_xFe_2O_4$ (x = 0.0, 0.3, 0.5, 0.7, 1.0), $CoFe_2O_4$, $BaTiO_3$ and $PbZr_{0.52}Ti_{0.48}O_3$ powders were synthesized by auto-combustion method. The composites were prepared by mixing the appropriate amounts of individual phases, pressing and conventional sintering. X-ray analysis, for individual phase and composites, indicated the formation of crystallized structure of $NiZnFe_2O_4$, $BaTiO_3$ and $PbZr_{0.52}Ti_{0.48}O_3$ without the presence of secondary phases or any impurities. SEM analyses indicated a formation of uniform grain distribution for ferromagnetic and ferroelectric phases and formation of two types of grains, polygonal and rounded, respectively. Magneto-dielectric effect was exhibited in all samples because of the applied stress occurring due to the piezomagnetic effect and the magnetic field induced the variation of the dielectric constant. For all samples the dielectric constant was higher in applied magnetic field. At the low frequency, the dispersion of dielectric losses appeared, while at the higher frequency the value of tan δ become constant (Maxwell-Wagner relaxation). Investigation of J-E relation between leakage and electric field revealed that both nickel zinc ferrite and composites have three different regions of conduction: region with ohmic conduction mechanism, region with the trap-controlled space charge limited current mechanism and region with space charge limited current mechanism.

Keywords: *multiferroic composites, combustion synthesis, dielectric properties*

I. Introduction

During the past 10 years, progressive research in the area of multiferroic materials has been conducted due to their promising properties and application. Multiferroics (MF) are defined as materials that exhibit more that one of the primary ferroic properties (magnetic, electric or elastic). As a result, they have spontaneous magnetization that can be switched by an external electric field, and spontaneous polarization that can be switched by an applied magnetic field. Coupling between ferroelectricity and ferromagnetism was found to be useful for multistate memories or memories with dual read-write mechanism [1], magnetic field sensors and electrically tunable microwave devices such as filters, oscillators and phase shifters [2,3]. Magneto-electric composites are still a topic of interest which can be seen from the current literature data [4–7]. There are two types of multiferroics: i) single phase multiferroics, in which one material possesses combined ferroelectric A-site and magnetic ordering on the B-site ($BiFeO_3$, $BiMnO_3$) and ii) composites consisting of two or more different phases, one with ferroelectric and another with magnetic ordering, such as $(Ni,Zn)Fe_2O_4$–$BaTiO_3$, $BaSrTiO_3$–$(Ni,Zn)Fe_2O_4$, $Ni(Co,Mn)Fe_2O_4$–$BaTiO_3$, $CoFe_2O_4$–$BaTiO_3$ [8–10].

Magneto-dielectric effect represents the influence of the magnetic induction (B) on the dielectric permittivity (ε) change. Magnetic field affects magnetic ordering in magneto-electric multiferroics and indirectly alters the dielectric permittivity. Magneto-capacitance (M_C) occurs due to the variation of dielectric constant (ε) and is observed to be proportional to the quadratic magneto-electric coefficient β [11]. The systems with heterogeneous structures, such as multiferroic composites, can be described with Maxwell-Wagner capacitor model consisting of two leaky capacitors connected in series. If there is a change of resistivity of any part of

*Corresponding authors: tel: +381 11 208 5057,
e-mail: *a.dzunuz@hotmail.com*

this heterogeneous system when the magnetic field is applied, it will affect the change of dielectric permittivity also.

According to the fact that composites consisting of ferroelectric and ferromagnetic phases exhibit a large value of M_C, it was interesting to investigate the background of the magneto-dielectric properties. Magneto-dielectric effect or magneto-capacitance effect was reported for a different kind of materials [11–14]. The magneto-capacitance (M_C) and magneto-losses (M_L) can be calculated from M–W equations [1,11]:

$$M_C = \frac{\varepsilon(H) - \varepsilon(0)}{\varepsilon(0)} \quad (1)$$

$$M_L = \frac{\tan\delta(H) - \tan\delta(0)}{\tan\delta(0)} \quad (2)$$

where $\varepsilon(H)$ is the value of dielectric permittivity when magnetic field is applied and $\varepsilon(0)$ dielectric permittivity at zero field.

Jigaeni *et al.* [11,12] synthesized $Sr_{0.5}Ba_{0.5}Nb_2O_6$-$Co_{1.2-x}Mn_xFe_1 \cdot 8\,O_4$ (SBN-CMFO) and confirmed the presence of ferroelectric behaviour of SBN and also presence of interfacial polarization. M_C was determined in two separate configurations of applied magnetic field and applied electric field where the applied magnetic and electric field are along the axis of a disc. They concluded that M_C in this case is larger than in the case where the magnetic field is along the radius of a disc while electric field is along the direction of disc axis. Also, M_C was positive for applied magnetic field parallel with the direction of strain and negative when the applied magnetic field was perpendicular to the direction of strain. Gridnev *et al.* [13] prepared two-layer PZT-MZF composites and concluded that value of magneto-dielectric response (MD) depends on the alternating electric field frequency, a volume fraction of the ferrite phase and magnetic field strength. They also observed that when the ferrite plate is placed in the magnetic field a deformation occurs because of a magnetostriction. After that the polarization appears because of the direct piezoelectric effect and with more applied magnetic field to the composite the more value of the polarization arises, which leads to the reduction in ε. Vijatovic Petrovic *et al.* [14] prepared two-phase composite ceramics that consisted of Sb doped barium titanate and nickel ferrite and confirmed the presence of magneto-dielectric effect in these composites. It is observed that the total dielectric permittivity of the composites has two contributions, one due to the stress induced variation of permittivity of the BT and other due to the magnetic field induced variation of dielectric permittivity of $NiFe_2O_4$ (NF). Sutar *et al.* [12] synthesized $Co_{0.9}Ni_{0.1}Fe_{2-x}Mn_xO_4$ (CNFMO where x = 0, 0.1, 0.2, 0.3, 0.4) and $Ba_{1-x}Sr_xTiO_3$ (BST where x = 0.2, 0.25, 0.3) and prepared CNFMO-BST composites with magneto-dielectric response. They observed that magneto-capacitance becomes maximum for 0.4CNFMO-0.6BST and concluded that M_C occurs because of strain induced change in polarization with applied magnetic field. They suggest that behaviour of magneto-capacitance could be understood in terms of the Landau thermodynamic theory.

The present paper reports the magneto-dielectric properties of: i) single phase materials: $Ni_{1-x}Zn_xFe_2O_4$ (NZF), $CoFe_2O_4$ (CF), $BaTiO_3$ (BT) and $PbZr_{0.52}Ti_{0.48}O_3$ (PZT) and ii) multiferroic composites: $Ni_{0.7}Zn_{0.3}F_2O_4$–$BaTiO_3$, $Ni_{0.7}Zn_{0.3}F_2O_4$–$PbZr_{0.52}Ti_{0.48}O_3$ and $CoFe_2O_4$–$PbZr_{0.52}Ti_{0.48}O_3$, prepared by the auto-combustion method. From the literature data it was observed that the NZF is characterized with high electrical resistivity, chemical stability and good electromagnetic properties while the BT possesses a high permittivity, low dielectric loss and high tunability [15–17]. CF, as a semi-hard material, has a good electrostrictive properties, large magnetocrystalline anisotropy, high coercivity, chemical stability and mechanical hardness, while PZT, with morphotropic phase boundary structure has excellent ferroelectric and piezoelectric properties [18,19]. The investigation of the magnetic field impact on dielectric properties of single phase materials and multiferroic composites was carried out. The structural, dielectric, magneto-dielectric and leakage current properties of these materials are reported and compared to literature data.

II. Experimental

2.1. Synthesis of ferroelectric and ferrite phases

Ferrite powders, Ni-Zn ferrites with the general formula $Ni_{1-x}Zn_xFe_2O_4$ (x = 0.0, 0.3, 0.5, 0.7, 1.0) and cobalt ferrite ($CoFe_2O_4$), were prepared by the auto-combustion method starting from metal nitrates ($Fe(NO_3)_3 \cdot 9\,H_2O$, $Ni(NO_3)_2 \cdot 6\,H_2O$, $Zn(NO_3)_2 \cdot 6\,H_2O$, $Co(NO_3)_2 \cdot 6\,H_2O$ and citric acid as a fuel. pH value was adjusted using ammonia solution. After the process of self-propagating reaction at 300 °C and thermal treatment at 1000 °C for 1 h complete transformation into pure ferrite phase (NZF or CF) was achieved. The powder was pressed at 196 MPa into pellets and sintered at 1250 °C for 4 h. Details of the auto-combustion method are reported earlier and can be found elsewhere [8,20].

Ferroelectric phases, barium titanate ($BaTiO_3$) and lead-zirconium titanate ($PbZr_{0.52}Ti_{0.48}O_3$) were also synthesized by the auto-combustion method. Starting reagents used for BT synthesis were $Ti(OCH(CH_3)_2)_4$ (TTIP), $C_6H_8O_7 \cdot H_2O$, $Ba(NO_3)_2$ and NH_4OH. The TTIP solution was added to a solution of previously heated citric acid at 60 °C. The resulting solution of titanium ortho-nitrate ($TiO(NO_3)_2$) was mixed with the solution of barium nitrate and citric acid. The temperature of 300 °C in the electrical calotte induced a self-propagation reaction and the obtained barium titanate precursor was further thermally treated at 900 °C

for 2 h [21]. Starting reagents used for PZT synthesis were: lead nitrate ($Pb(NO_3)_2$), zirconium (IV) oxynitrate hydrate ($ZrO(NO_3)_2 \cdot H_2O$), titanium isopropoxide $Ti(OCH(CH_3)_2)_4$, $C_6H_8O_7 \cdot H_2O$ and NH_4OH. The obtained PZT precursor powder was calcined at 800 °C for 2 h in order to obtain a pure PZT.

The synthesized ferromagnetic and ferroelectric powders were later used for the preparation of $x Ni_{0.7}Zn_{0.3}Fe_2O_4$–$(1-x)BaTiO_3$ (x = 0.3, 0.5, 0.7), $x Ni_{0.7}Zn_{0.3}Fe_2O_4$–$(1-x)PbZr_{0.52}Ti_{0.48}O_3$ (x = 0.1, 0.2) and $x CoFe_2O_4$–$(1-x)PbZr_{0.52}Ti_{0.48}O_3$ (x = 0.1, 0.2) composites.

2.2. Preparation of multiferroic composites

Several series of multiferroic composites were prepared by mixing and homogenizing ferroelectric and ferrite phases. First, the NZF and BT powders were used to produce MF composites with the following formula $x Ni_{0.7}Zn_{0.3}Fe_2O_4$–$(1-x)BT$ (x = 0.3, 0.5, 0.7). The MF composites are formed as pellets pressed at 196 MPa. Different sintering temperatures, 1120 °C and 1170 °C, were used to obtain composites with only two phases and the highest possible densities to improve the dielectric properties of MFs.

Secondly, the NZF-PZT and CF-PZT composites were made in the same way as previous, but under different sintering conditions (1150–1170 °C).

2.3. Methods and characterization of ceramics

The phase and crystal structure analysis were carried out by an X-ray diffraction technique (Model Rigaku RINT 2000, CuKα radiation). Scanning electron microscope (SEM) (Model TESCAN SM-300) was used for the microstructural characterization of the ceramics. Silver electrodes were applied on both surfaces of the ceramics for the electrical measurements. Magnetodielectric properties of studied materials were investigated using custom built set-up, where the dielectric permittivity at zero field and with applied magnetic field of 0.5 T were measured using LCR meter (model 9593-01, HIOKI HITESTER). To study leakage current behaviour of the ceramics, current density versus electric field was measured using a Keathley Source Meter with and without the applied magnetic field (0.5 T).

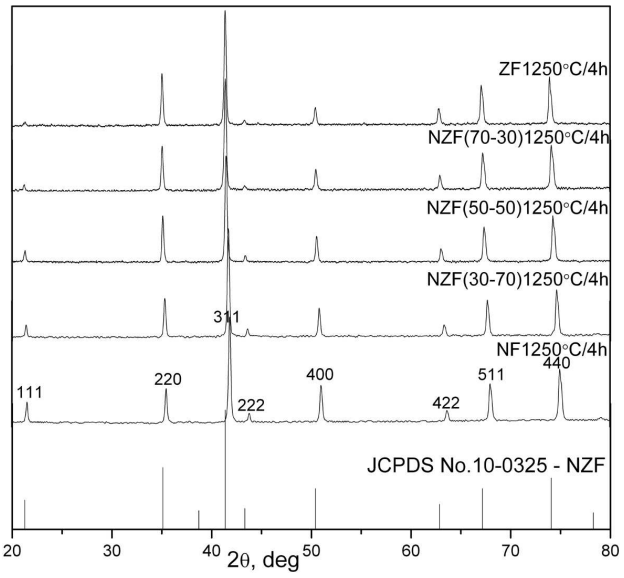

Figure 1. XRD patterns of NZF ferrites sintered at 1250 °C

III. Results and discussion

3.1. Structural characterization

Figure 1 shows XRD spectra of $Ni_{1-x}Zn_xFe_2O_4$ (x = 0.0, 0.3, 0.5, 0.7, 1.0) sintered at 1250 °C for 4 h. The formation of the spinel cubic structure of Ni-Zn ferrite system is evident. All the peaks correspond to nickel zinc ferrite phase which was confirmed by the existence of the appropriate reflections, identified using the JCPDS file No. 10-0325. The investigation of the magnetic properties of nickel zinc ferrite [20], showed that the optimal molar ratio between nickel and zinc, for the achievement of good magnetic properties, was 70/30. Thus, in our previous paper [21] the NZF with molar ratio Ni/Zn = 0.70/0.30 was used for the production of the multiferroic composite materials with ferroelectric phases, BT and PZT.

From Fig. 2 it can be observed that the obtained BT powder possessed tetragonal crystal structure (JCPDS file No. 05-0626), without any secondary phases. This figure also shows the XRD spectrum of the composites $x Ni_{0.7}Zn_{0.3}Fe_2O_4$–$(1-x)BT$ (x = 0.7, 0.5, 0.3) which confirmed that both phases (spinel and perovskite) were present in the composites. The different sintering temperatures were applied in order to obtain composites without secondary phases and with the highest possible densities for conventional sintering regime. From the XRD diagrams for composites presented in Fig. 2, it can be observed that the intensity of the peaks that

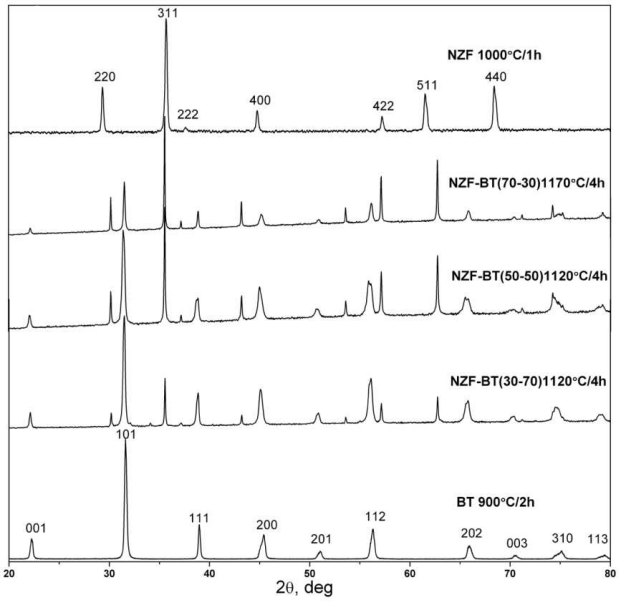

Figure 2. XRD patterns of multiferroic composite ceramics and barium titanate and nickel zinc ferrite powders

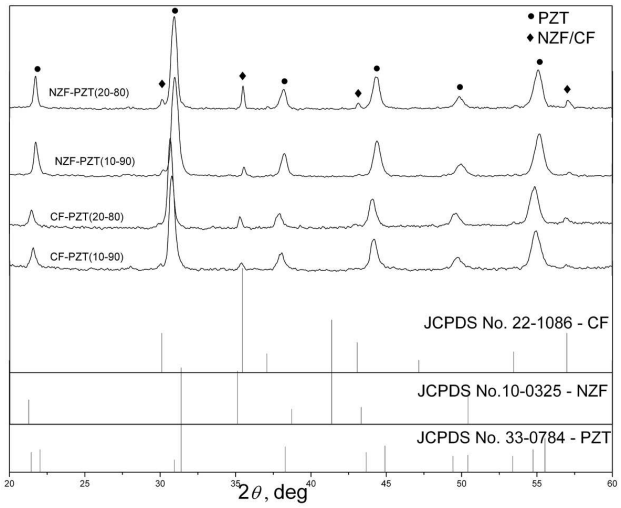

Figure 3. XRD patterns of NZF-PZT and CF-PZT ceramics

correspond to the BT phase increased with the increase of the molar ratio of BT phase. Similarly, Fig. 3 presents XRD diagrams of the NZF-PZT and CF-PZT composites in which all diffraction peaks correspond to the cubic spinel structure of $CoFe_2O_4$ and $Ni_{0.7}Zn_{0.3}Fe_2O_4$ and perovskite structure of $PbZr_{0.52}Ti_{0.48}O_3$ [22].

Morphology of the BT and NZF(70-30) powders was presented in Fig. 4. From SEM micrographs it could be seen that both BT and NZF powders are highly agglomerated, with small primary particle size (<200 nm). Since the homogenization of the powders was performed in the planetary ball mill, agglomeration was diminished in the certain percentage and similar particle sizes allowed good homogenization of the phases in the composite material.

Microstructures of the MF ceramics consisting of NZF and BT phases were presented in Fig. 5. Microstructure analysis showed that all BT based MFs contained polygonal nickel zinc ferrite grains and more rounded grains of barium titanate. Homogeneous phase distribution was noticed in all formed nanosized ceramics in which the average grain size was around 100–300 nm.

SEM images of the sintered NZF-PZT and CF-PZT composites presented in Fig. 6 showed more spherical and smaller PZT grains and polygonal grains of NZF and CF. Grain size of the ferroelectric phase in both types of MFs was smaller due to the fact that they need much higher sintering temperature for significant grain growth. According to the available literature, BT and PZT have been usually sintered at 1200–1350 °C in order to get highly dense microstructure which will enable good electrical properties of the material [23,24]. However, the formation of secondary phases at the in-

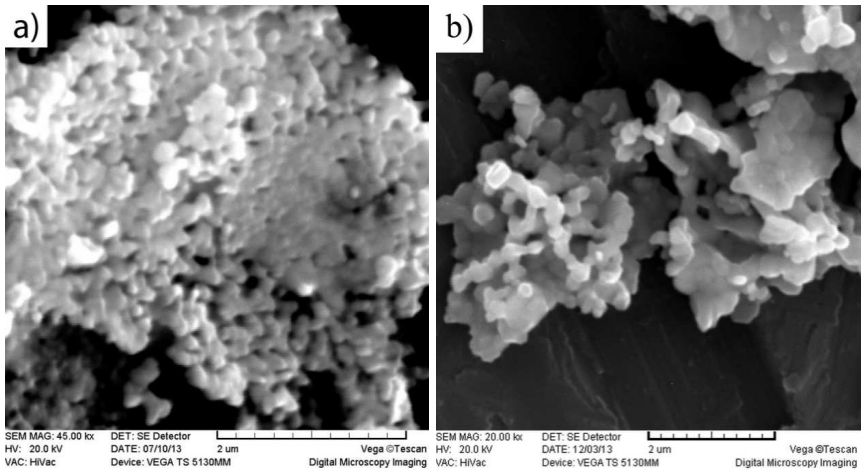

Figure 4. SEM images of: a) BT and b) NZF powder

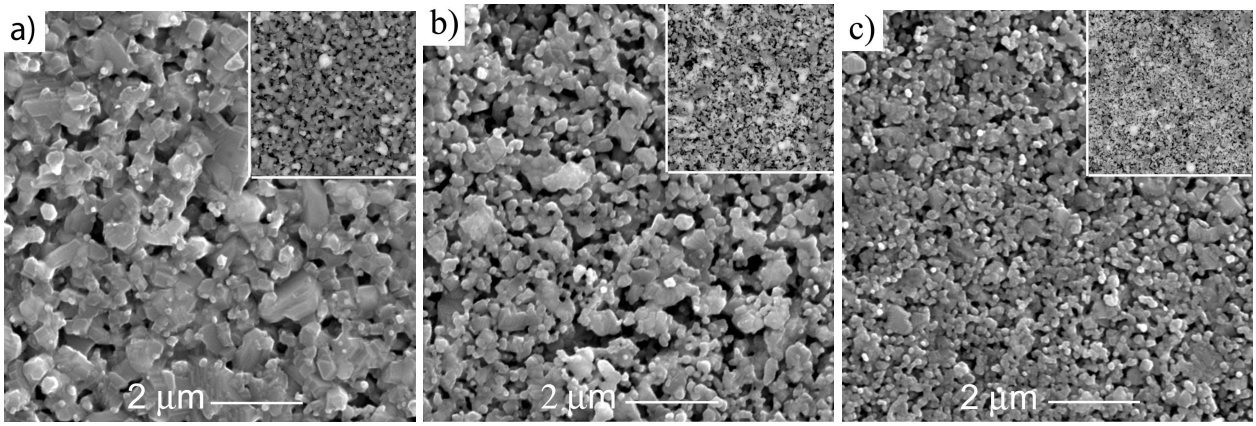

Figure 5. SEM images of: a) NZF-BT(70-30), b) NZF-BT(50-50) and c) NZF-BT(30-70) ceramics

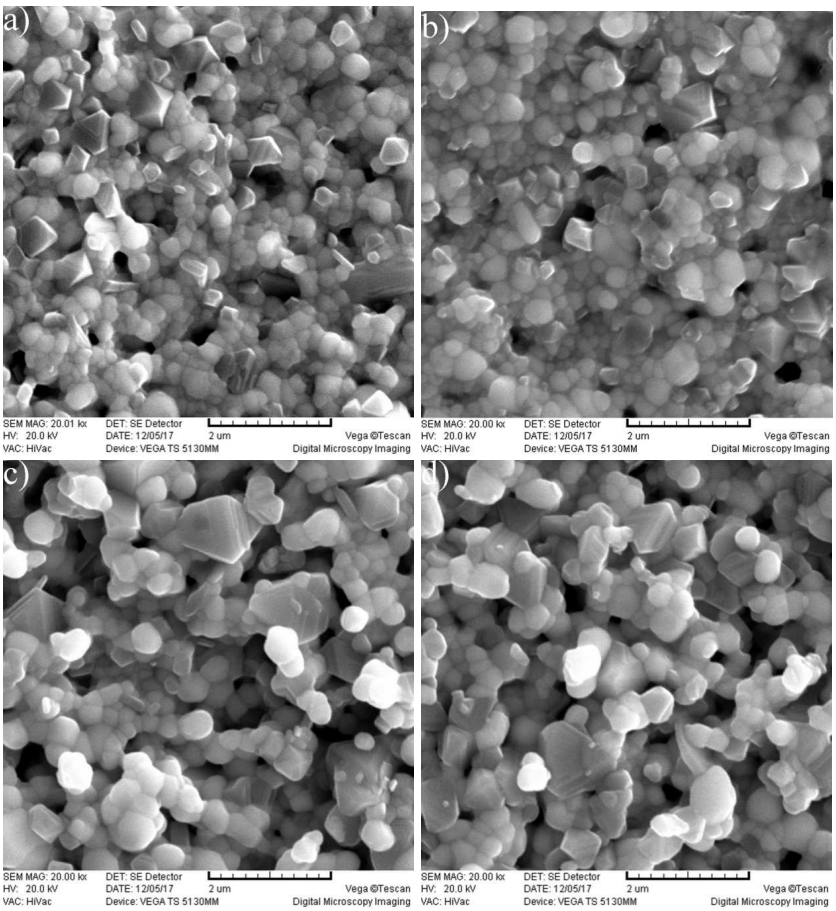

Figure 6. SEM images of: a) NZF-PZT(10-90), b) NZF-PZT(20-80), c) CF-PZT(10-90), CF-PZT(20-80) ceramics

terfaces in this type of materials was noticed at much lower temperatures [8] and therefore, the optimization of sintering process was very important in this segment of MFs preparation. It is important to stress that these samples are porous and the effective distance between the electrodes can vary, which can complicate the interpretation of the experimental data obtained by electrical characterization.

3.2. Dielectric and magneto-dielectric properties

In the MF materials magnetic field affects magnetic ordering, but it can also indirectly modify the dielectric permittivity of the material. The existence of the magneto-dielectric effect was analysed by applying an external static magnetic field and by measuring the dielectric permittivity and dielectric losses vs. frequency dependences. Figures 7–9 show the variation of dielectric permittivity and dielectric losses as a function of $\log f$ with and without applied magnetic field of 10 kOe in the frequency range from 42 Hz to 1 MHz for the NZF ferrites and all composite ceramics.

The ε–$\log f$ and $\tan\delta$–$\log f$ dependences presented in Fig. 7 for the NZF magnetic materials do not differ much with and without applied magnetic field, but the characteristic relaxations were noticed in the frequency range from 100 to 400 Hz. However, values of

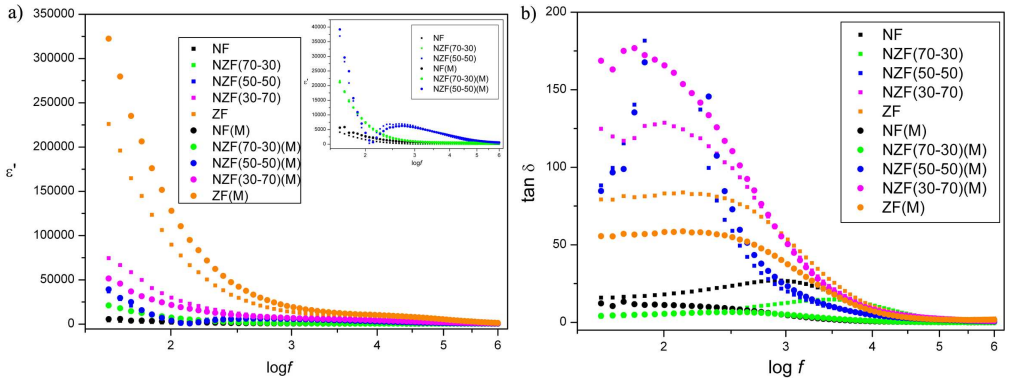

Figure 7. a) ε' as a function of $\log f$, b) $\tan\delta$ as a function of $\log f$ for NZF magnetic materials

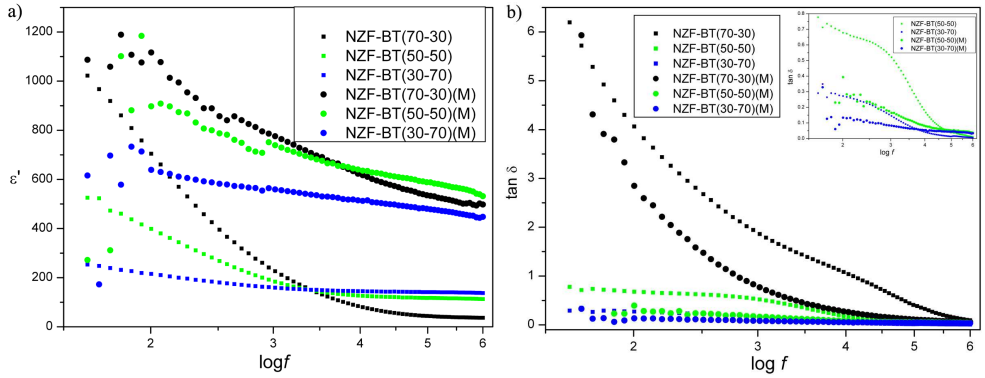

Figure 8. a) ε' as a function of log$f$, b) tan δ as a function of log$f$ for NZF-BT composite materials

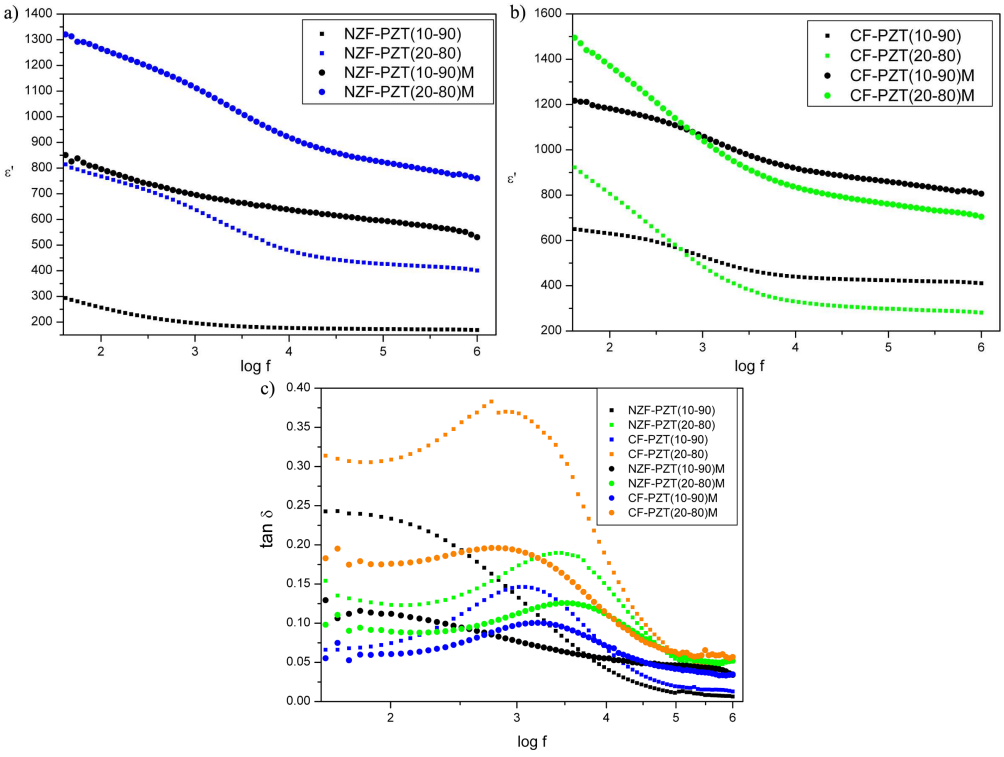

Figure 9. a) and b) ε' as a function of log$f$, c) tan δ as a function of log$f$ for NZF-PZT and CF-PZT composites materials

the ε measured with applied magnetic field were slightly higher in comparison with ε measured without the magnetic field in the whole frequency region. M_C decreased with the increase of the molar ratio of Zn for all investigated frequencies (Fig. 10a). It is observed that M_C decreased with frequency decrease for all samples except in the case of $ZnFe_2O_4$ (ZF) and with positive sign, till 1000 Hz. Below this frequency value of the M_C becomes negative which was reported earlier for some ferrites with spinel crystal structure [25,26].

On the other hand, regarding the MF composites, there are two effects that can have the impact on the dielectric permittivity of these materials when they are placed in the magnetic field. Since the magnetic field is applied along the disc axis, it was proposed that the first possible effect is stress induced. Due to the influence of magnetic field (magnetostriction induced) on the BT and PZT materials which have piezoelectric properties, M_C can be positive or negative. For all investigated composites, NZF-BT and NZF/CF-PZT, the dielectric permittivity was higher when magnetic field was applied (Figs. 8 and 9) and exhibited positive values of M_C (Fig. 10). Depending on the composition, the M_C can be quite large, indicating also large ME coupling between ferroelectric and ferromagnetic phase. Magneto-capacitance effect found in the investigated composites was significantly higher in comparison with M_C obtained for multiferroic composites reported by others [25,27]. The other effect occurred possibly because of the presence of interfacial polarization caused by the difference between the resistivity and dielectric permittivity of ferroelectric and ferromagnetic phases in the composites. The presence of magneto-capacitance effect in the BT-NZF and NZF/CF-PZT systems may be attributed to the influence of external magnetic field on the magnetic arrangement in the ferrite phase and further on the inter-

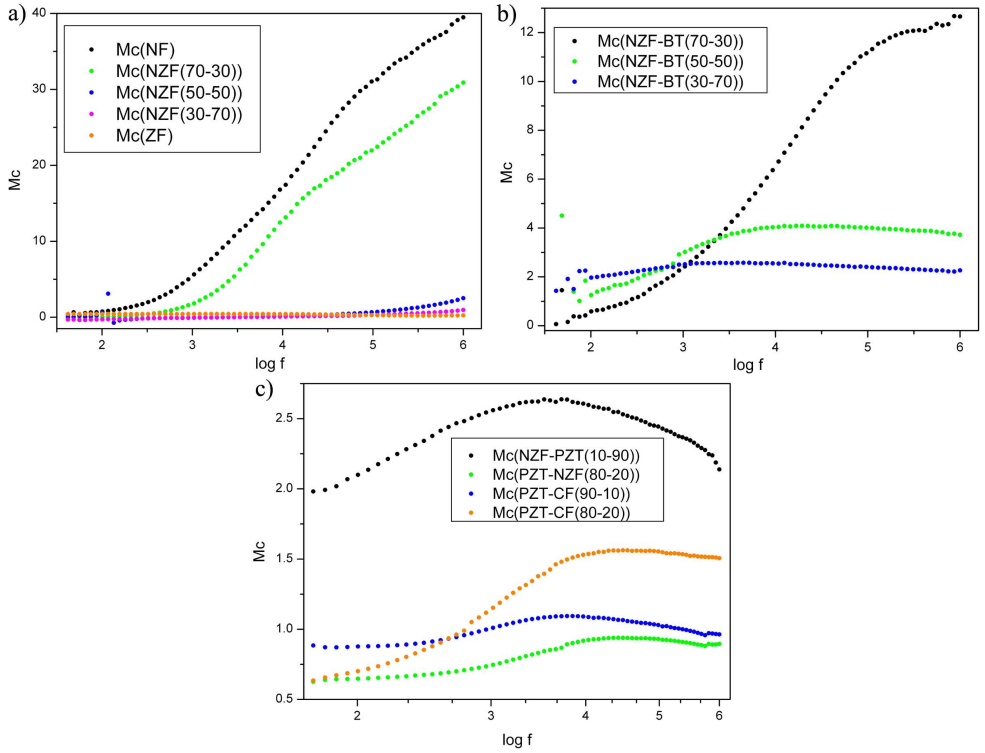

Figure 10. M_C **as a function of** $\log f$ **for NZF, NZF-BT, NZF-PZT and CF-PZT composites**

face between BT and NZF. These changes in the magnetic ordering can cause the deformation in the ferrite phase and mechanically activate the piezoelectric BT and PZT [28]. In the NZF-BT composites, higher concentration of BT phase causes higher piezoelectric effect and higher polarization, but smaller dielectric permittivity and magneto-dielectric effect. Nevertheless, based on the measurements for pure magnetic materials (Fig. 7a), the contribution of magnetic phase on the M_C increase was also expected and proved. On the other hand, the difference of magneto-capacitance between composites CF-PZT and NZF-PZT was noticed possibly due to different conductivities of the ferrites [29–31]. These differences in conductivities resulted in the deviation of the real part of dielectric permittivity (which caused a different value of M_C) via the Maxwell-Wagner relaxation process. To confirm which types of polarons (large or small) determine conduction we have examined the variation of conductivity with frequency at room temperature. AC conductivity, σ_{AC} is calculated from the dielectric constant and dielectric losses using the relation:

$$\sigma_{AC} = \varepsilon' \varepsilon_0 \omega \tan\delta \tag{3}$$

where ε_0 is the vacuum permittivity and ω is the angular frequency.

The dependence of $\log(\sigma_{AC} - \sigma_{DC})$ (Fig. 11) *vs.* $\log \omega^2$ present plots that are straight lines, indicating that the conduction in the MF composites is the result of small polarons movement [32].

The variation of dielectric losses with frequency in the frequency range from 40 Hz to 1 MHz for NZF-BT and NZF/CF-PZT composites is shown in Figs. 8b. and 9c. Dielectric loss ($\tan\delta$) of the investigated composites decreased when magnetic field was applied. At the low frequency, the dispersion of the dielectric losses appeared, while at the higher frequency the value of $\tan\delta$ became constant. This may be due to the presence of dipoles which disappeared at higher frequencies because of the influence of an applied magnetic field. In the composites this behaviour is conditioned because of the heterogeneous structure of the composite based on the Maxwell-Wagner relaxation mechanism [33]. A high value of dielectric losses was observed for the samples ZF, NZF(50-50) and NZF(30-70), i.e. samples with more Zn. This can be attributed to the impact of electrons hoping between mobile charges like Fe^{2+} and Fe^{3+} resulting in consumption of energy. The MF compos-

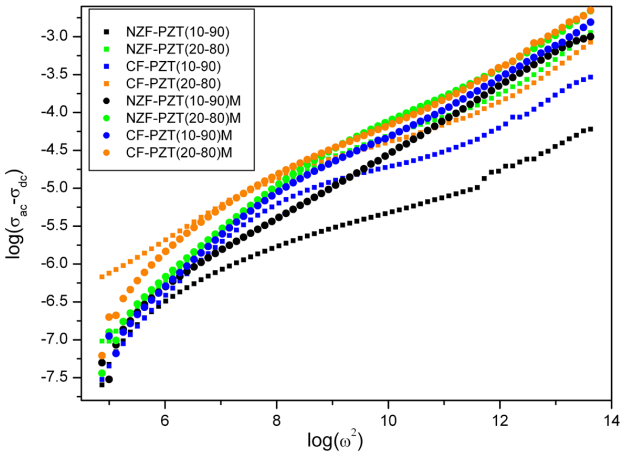

Figure 11. Variation of $\log(\sigma_{AC} - \sigma_{DC})$ **with** $\log \omega^2$ **for NZF-PZT and CF-PZT**

ite samples NZF-BT(50-50) and NZF-BT(30-70) (Fig. 8b) have significantly lower value of dielectric losses in comparison with the NZF-BT(70-30) composite. In the NZF-PZT and CF-PZT composites, the relaxation of dielectric losses was present and losses were much lower in magnetic field, which was not the case with the NZF-BT samples. Figure 10 presents significant change in M_C value in the lower frequency region (<6 kHz) which can be attributed to the magneto-dielectric effect combined with Maxwell-Wagner effect [34].

When an electric field exists between electrodes, leakage current appears if the ferroelectric ceramics is semiconducting. In order to study conductivity mechanism of the nickel zinc ferrite and NZF-BT and NZF/CF-PZT composites, leakage-current density, J, was measured at room temperature as a function of static electric-field E (Fig. 12). Slope of the curve in logarithmic plot, $\log J$ versus $\log E$, determine the nature of conduction [35]. There are three possible mechanisms of conduction [36,37]: ohmic conduction mechanism which represents the linear relation between leakage and electric field, with the conductivity Γ:

$$J_i = \Gamma E_i \tag{4}$$

space charge limited conduction (SCLC) which represents a quadratic dependency on the electric field, with the carrier mobility μ and the relative dielectric constant ε_r:

$$J_i = 9/8\mu\varepsilon_r E E_i \tag{5}$$

and the Schottky emission with the exponential dependency on to the electric field.

The measurements were performed with and without magnetic field for all samples. For the NZF samples, nearly straight lines with two distinct slope regions can be noticed from $\log J$ versus $\log E$. In low field region, slope was found to be between 1 and 1.5 which suggested the existence of ohmic conduction mechanism in these samples. In high field region the slope is almost always between 1.5 and 2 which pointed on the existence of space-charge-limited-conduction (SCLC) mechanism. Also, leakage current was lower for the NF sample in comparison with the NZF samples. This suggests that concentration of free charge carries, in this case oxygen vacancies formed due to Fe^{3+} reduction to Fe^{2+} (Eqs. 6 and 7), were being reduced in samples with more nickel [38]. In the real systems, the current increases with finite slope and with the value larger than 2. This mechanism is described by trap-controlled SCLC mechanism.

$$Fe^{x}_{Fe} + e' \longleftrightarrow Fe'_{Fe} \tag{6}$$

$$O^{x}_{O} \longleftrightarrow V_{O}^{\bullet\bullet} + 2\,e' + \frac{1}{2}\,O_2 \tag{7}$$

Figures 12c and 12d show J-E dependence for the investigated MF composites. The MFs with more ferroelectric phase, BT and PZT possessed higher values of leakage current density. It can be explained by the fact that BT and PZT are much more resistive in comparison with ferrite phases (NZF and CF). Two different regions of conduction were present here: i) region with ohmic conduction mechanism where the thermally generated free carriers density was higher than the density of injected charge carriers; ii) region with SCLC mechanism where the concentration of injected carriers was higher than thermally generated free carriers and dominate the conduction. In the case of the NZF-PZT and CF-PZT

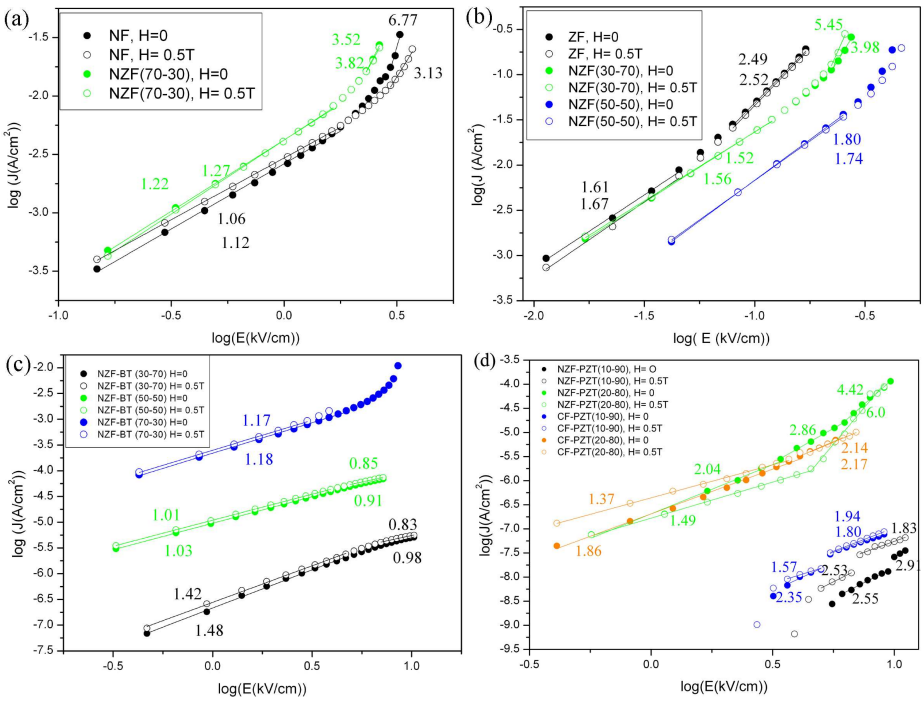

Figure 12. Leakage-current density, J as a function of static electric-field, E for NZF, NZF-BT and PZT-NZF, CF samples

composites besides above mentioned two regions, the third region of conduction was also noticed. According to literature data, it was proposed that this region was based on the trap-controlled SCLC mechanism where all the traps will be filled with the injected carriers [39].

IV. Conclusions

Ferromagnetic (NZF and CF) and ferroelectric (BT and PZT) powders were successfully synthesized using auto-combustion reaction method. Multiferroic composites were prepared by mixing ferromagnetic and ferroelectric phase, followed by pressing and sintering under different conditions. XRD confirmed the presence of individual phases without secondary phases in powder samples and biphase multiferroic composites ceramics. SEM analysis indicated the formation of powders consisting of small rounded primary particles (<200 nm) with high level of agglomeration. Also, microstructure analysis showed the formation of sintered ceramic composites with grains of different shapes with sizes around 300 nm.

The ε'-f measurements pointed that the applied external magnetic field had influence on the dielectric spectra, indicating the magneto-dielectric effect in the system, for all investigated ceramics. For NZF samples, the M_C decreased with the increase of the molar ratio of Zn for all investigated frequencies. Dielectric permittivity of the composites was influenced by two effects: one which was stress induced by the influence of magnetic field (magnetostriction induced) and the other one appeared due to the presence of interfacial polarization in the composites. Dielectric losses ($\tan\delta$) of the investigated composites decreased when magnetic field was applied. Leakage current density measurements suggested the change of the conduction mechanism from SCLC to ohmic type. Leakage current density for the NZF samples was lower in comparison with the NF ceramics, possibly due to the reduced concentration of oxygen vacancies in samples with more nickel. The composites with higher concentration of ferroelectric phase, BT and PZT, had higher value of leakage current density because BT and PZT have greater resistance in comparison with ferrite phase. The analysis of the dependence of the leakage-current density on the applied magnetic field showed a difference between the results obtained with and without the magnetic field.

Acknowledgement: The authors gratefully acknowledge the financial support of the Ministry of Education, Science and Technological Development of the Republic of Serbia (project III 45021).

References

1. G. Catalan, "Magnetocapacitance without magnetoelectric coupling", *Appl. Phys. Lett.*, **88** (2006) 102902.
2. S. Archary, O. Jayakumar, A. Tyagi, *Functional Materials*, p. 159, Elsevier Insights, USA, 2012.
3. H. Schmid, "Multi-ferroic magnetoelectric", *Ferroelectric*, **132** (1994) 317–338.
4. S. Babu, J. Hsu, Y. Chen, J. Lin, "Magnetoelectric response in lead-free multiferroic $NiFe_2O_4$-$Na_{0.5}Bi_{0.5}TiO_3$ composites", *J. Appl. Phys.*, **109** [7] (2011) D904.
5. A. Fawzi, A. Sheikh, V. Mathe, "Composition dependent electrical, dielectric, magnetic and magnetoelectric properties of (x)$Co_{0.5}Zn_{0.5}Fe_2O_4$ + (1-x)PLZT composites", *J. Alloy. Compd.*, **493** (2010) 601–608.
6. N. Spaldin, M. Fiebig, "The renaissance of magnetoelectric multiferroics", *Science*, **309** (2005) 391–392.
7. S. Dong, J. Li, D. Viehland, "Magnetoelectric coupling, efficiency, and voltage gain effect in piezoelectric piezomagnetic laminate composites", *J. Mater. Sci.*, **41** (2006) 97–106.
8. A. Dzunuzovic, M. Vijatovic Petrovic, B. Stojadinovic, N. Ilic, J. Bobic, C. Foschini, M. Zaghete, B. Stojanovic, "Multiferroic (NiZn)Fe_2O_4-$BaTiO_3$ composites prepared from nanopowders by auto-combustion method", *Ceram. Int.*, **41** (2015) 13189–13200.
9. R. Mondal, B. Murty, V. Murthy, "Dielectric, magnetic and enhanced magnetoelectric response in high energy ball milling assisted BST-NZF particulate composite", *Mater. Chem. Phys.*, **167** (2015) 338–346.
10. R. Pandya, U. Joshi, O. Caltun, "Microstructural and electrical properties of barium strontium titanate and nickel zinc ferrite composites", *Procedia Mater. Sci.*, **10** (2015) 168–175.
11. S. Jigajeni, A. Tarale, D. Salunkhe, P. Joshi, S. Kulkarni, "Dielectric, magnetoelectric and magnetodielectric properties in CMFO-SBN composites", *Ceram. Int.*, **39** (2013) 2331–2341.
12. M. Sutar, A. Tarale, S. Jigajeni, S. Kulkarni, V. Reddy, P. Joshi, "Magnetoelectric and magnetodielectric effect in $Ba_{1-x}Sr_xTiO_3$ and $Co_{0.9}Ni_{0.1}Fe_{2-x}Mn_xO_4$ composites", *Solid State Sci.*, **14** (2012) 1064–1070.
13. S. Gridnev, A. Kalgin, V. Chernykh, "Magnetodielectric effect in two-layer magnetoelectric PZT-MZF composite", *Integr. Ferroelectr.*, **109** (2009) 70–75.
14. M. Vijatovic Petrovic, R. Grigalaitis, A. Dzunuzovic, J. Bobic, B. Stojanovic, R. Salasevicius, J. Banys, "Positive influence of Sb doping on properties of di-phase multiferroics based on barium titanate and nickel ferrite", *J. Alloy. Compd.*, **749** (2018) 1043–1053.
15. L. Mitoseriu, "Magnetoelectric phenomena in single-phase and composite systems", *Bol. Soc. Esp. Ceram.*, **44** [3] (2005) 177–184.
16. M. Botello-Zubiate, D. Bueno-Baques, J. deFrutos, L. Fuentes, J. Matutes-Aquino, "Synthesis and magnetoelectric characterization of cobalt ferrite-barium titanate composites using a new pulsed magnetic field method", *Integr. Ferroelectr.*, **83** (2006) 33–40.
17. C. Nan, M. Bichurin, S. Dong, D. Viehland, G. Srinivasan, "Multiferroic magnetoelectric composites: Historical perspective status and future directions", *J. Appl. Phys.*, **103** (2008) 031101.
18. N. Hosni, K. Zehani, T. Bartoli, L. Bessais, H. Maghraoui-Meherzi, "Semi-hard magnetic properties of nanoparticles of cobalt ferrite synthesized by the co-precipitation process", *J. Alloy. Compd.*, **694** (2017) 1295–1301.
19. J. Peng, M. Hojamberdiev, H. Li, D. Mao, Y. Zhao, P. Liu, J. Zhou, G. Zhu, "Electrical, magnetic, and direct and converse magnetoelectric properties of (1-x)$Pb(Zr_{0.52}Ti_{0.48})O_3$-(x)$CoFe_2O_4$ (PZT-CFO) mag-

netoelectric composites", *J. Magn. Magn. Mater.*, **378** (2015) 298–305.
20. A. Džunuzović, N. I.Ilić, M. Vijatović Petrović, J .Bobić, B. Stojadinović, Z. Dohčević-Mitrović, B. Stojanović, "Structure and properties of Ni-Zn ferrite obtained by auto-combustion method", *J. Magn. Magn. Mater.*, **374** (2015) 245–251.
21. A. Dzunuzovic, M. Vijatovic Petrovic, J. Bobic, N. Ilic, M. Ivanov, R. Grigalaitis, J. Banys, B. Stojanovic, "Magnetoelectric properties of $xNi_{0.7}Zn_{0.3}Fe_2O_4$-(1-x)$BaTiO_3$ multiferroic composites", *Ceram. Int.*, **44** (2018) 683–694.
22. J. Bobić, M. Ivanov, N. Ilić, A. Dzunuzović, M. Vijatović Petrović, J. Banys, A. Ribic, Z. Despotovic, B. Stojanovic, "PZT-nickel ferrite and PZT-cobalt ferrite comparative study: Structural, dielectric, ferroelectric and magnetic properties of composite ceramics", *Ceram. Int.*, **44** (2018) 6551–6557.
23. M. Vijatovic Petrovic, J. Bobic, J. Banys, B. Stojanovic, "Electrical properties of antimony doped barium titanate ceramics", *Mater. Res. Bull.*, **48** (2013) 3766–3772.
24. Dipti, J. Juneja, S. Singh, K. Raina, C. Prakash, "Enhancement in magnetoelectric coupling in PZT based composites", *Ceram.Int.*, **41** (2015) 6108–6112.
25. S. Gridnev, A. Kalgin, V. Chernykh, "Magnetodielectric effect in two-layer magnetoelectric PZT-MZF composite", *Integr. Ferroelectr.*, **109** (2009) 70–75.
26. M. Salunkhe, S. Jigajeni, M. Sutar, A. Tarale, P. Joshi, "Magnetoelectric and magnetodielectric effect in CFMO-PBT nanocomposites", *J. Phys. Chem. Solids*, **74** (2013) 388–394.
27. P. Mandal, T. Nath, "Enhanced magnetocapacitance and dielectric property of $Co_{0.65}Zn_{0.35}Fe_2O_4$-$PbZr_{0.52}Ti_{0.48}O_3$ magnetodielectric composites", *J. Alloy. Compd.*, **599** (2014) 71–77.
28. S. Singh , N. Kumar , R. Bhargava, M. Sahni , K. Sung, J. Jung, "Magnetodielectric effect in $BaTiO_3$/$ZnFe_2O_4$ core/shell nanoparticles", *J. Alloy. Compd.*, **587** (2014) 437–441.
29. T. Takenaka, H. Nagata, Y. Hiruma, Y. Yoshii, K. Matumoto, "Lead-free piezoelectric ceramics based on perovskite structures", *J. Electroceram.*, **19** (2007) 259–265.
30. J. Gao, D. Xue, W. Liu, C. Zhou, X. Ren, "Recent progress on $BaTiO_3$-based piezoelectric ceramics for actuator applications", *Actuators*, **6** [3] (2017) 24.
31. G.H. Jonker, "Analysis of the semiconducting properties of cobalt ferrite", *J. Phys. Chem. Solids*, **9** (1959) 165–175.
32. R. Mahajan, K. Patankar, M. Kothale, S. Patil, "Conductivity, dielectric behaviour and magnetoelectric effect in copper ferrite-barium titanate composites", *Bull. Mater. Sci.*, **23** (2000) 273–279.
33. K. Patankar, S. Joshi, B. Chougule, "Dielectric behaviour in magnetoelectric composites", *Phys. Lett. A*, **346** (2005) 337–341.
34. G. Catalan, "Magnetocapacitance without magnetoelectric coupling", *Appl. Phys. Lett.*, **88** (2006) 102902.
35. C. Chung, J.Lin, J.Wu, "Influence of Mn and Nb dopants on electric properties of chemical-solution-deposited $BiFeO_3$ films", *Appl. Phys. Lett.*, **88** (2006) 242909.
36. H. Du, W. Liang, Y. Li, M. Gao, Y. Zhang, C. Chen, Y. Lin, "Leakage properties of $BaTiO_3$ thin films on polycrystalline Ni substrates grown by polymer-assisted deposition with two-step annealing", *J. Alloy. Compd.*, **645** (2015)166–171.
37. V. Janardhanam, Y. Park, K. Ahn, C. Choi, "Carrier transport mmechanism of Se/n-type Si Schottky diodes", *J. Alloy. Compd.*, **534** (2012) 37–41.
38. S. Godara, B. Kumar, "Effect of Ba-Nb co-doping on the structural, dielectric, magnetic and ferroelectric properties of $BiFeO_3$ nanoparticles", *Ceram. Int.*, **41** (2015) 6912–6919.
39. S. Park, J. Lee, J. Jang, H. Rhu, H. Yu, B. You, C. Kim, K. Kim, Y. Cho, S. Baik, W. Lee, "In situ control of oxygen vacancies in TiO_2 by atomic layer deposition for resistive switching devices", *Nanotechnology*, **24** (2013) 295202.